A DROPLET IMPACT MODEL FOR AGENT TRANSPORT IN ENGINE NACELLES[†]

Paul E. DesJardin
Sandia National Laboratories
Fire Science and Technology
P.O. Box 5800
Albuquerque, NM 87125-0836
Tel: 505-844-7740; FAX: 505-844-8251
E-mail: pedesja@sandia.gov

Cary Presser
Chemical Science and Technology Laboratory
National Institute of Standards and Technology
Gaithersburg, MD 20899-8360

Peter J. Disimile and James R. Tucker
USAF 46 TW Aerospace Survivability and Safety Flight
Wright-Patterson Air Force Base, OH

ABSTRACT

The overall objective of this research is to gain fundamental knowledge of fire-suppression agent transport in the cluttered environments of aircraft engine nacelles (*i.e.*, hydraulic and electrical lines, mounting brackets, etc.). A new generation of Halon replacements includes chemical suppressants with high boiling points that will exist in a liquid phase at discharge. The release of these agents in confined spaces may result in the impact of droplets with nearby solid surfaces and inhibit the effectiveness of the agent. The focus of the current effort is to develop a model to account for these effects in a Lagrangian modeling framework for spray transport. The impact model is formulated using mass and energy conservation principles along with established empirical correlations for breakup of individual droplets. Results are presented for 1 mm diameter HFE-7100 liquid droplets impacting into a circular cylinder for several velocities spanning the impact regimes of droplet adhesion, bouncing and breakup.

INRODUCTION

A new generation of Halon replacements includes chemical suppressants that have high boiling points and theoretically may exist in liquid upon discharge. Release of these agents into engine nacelles under high pressure will result in the impact of droplets on nearby solid surfaces, and severely limit the ability of the suppressant to be advected to a fire. Accounting for these effects will therefore be important in the numerical modeling of agent transport in these spaces.

Due to its wide range of applicability, several studies have been conducted on droplet impact and discussed in the excellent reviews on the subject by Healy *et al*. [1] and Rein

[†] This work was performed in part at Sandia National Laboratories, a multiprogram laboratory operated by Sandia Corporation, a Lockheed-Martin Company, for the U.S. Department of Energy under contract DE-AC04-94AL85000.

[2]. Previous work on droplet impact has largely focused on the spreading rate and maximum splat size of individual droplets as a function of surface temperature, roughness, wetting conditions and initial droplet Weber number. These studies include detailed high-speed photography measurements and numerical simulations of water [3,4,5,6,7,8,9,10], heptane [11,12], molten metals [13,14] and, more recently, liquid fire suppressants [15,16]. However, to the authors' knowledge, there has not been a simplified phenomenological model for droplet impact that is suitable for numerical simulation of sprays involving thousands of droplets. The objective of this study is to develop such a model for use in general purpose CFD codes for prediction of liquid agent dispersal in spaces including aircraft engine nacelles.

The formulation of a droplet impact model is presented in the following sections. Results are provided for a stream of 1 mm HFE-7100 droplets impacting a cylinder for three impact regimes resulting in droplet rebound, sticking, and shattering. Conclusions are then drawn and recommendations for future work are outlined.

PHENOMENOLOGICAL DROPLET IMPACT MODEL FORMULATION

A droplet impact model is formulated using simple mass and energy conservation principles at three thermo-physical droplet states shown below in Figure 1.

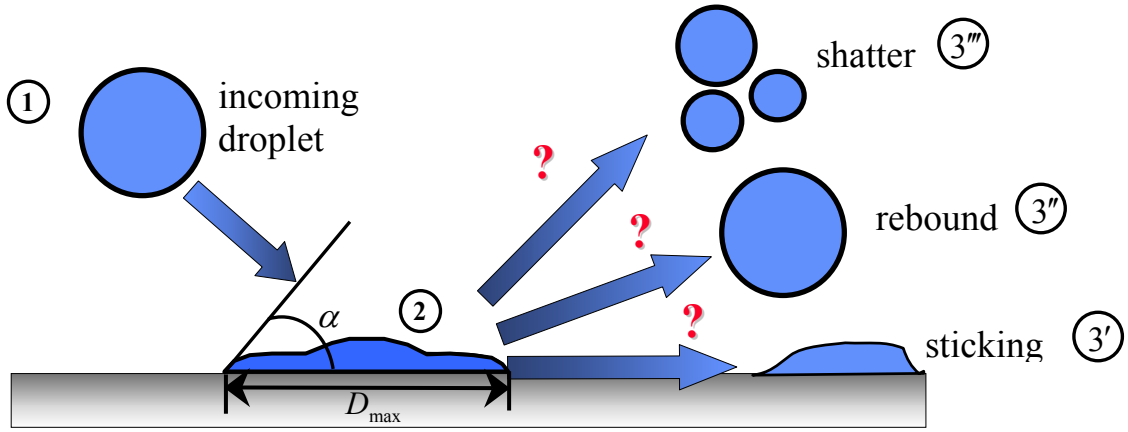

Figure 1: Configuration states during droplet impact consisting of (1) pre-impact, (2) impact and (3) post-impact (*i.e.*, sticking, rebound or shattering).

State (1) corresponds to the pre-impact state where the droplet is assumed to be spherical in shape and the mass and energy of the droplet can be expressed as follows.

$$\begin{aligned} m &= \rho^{(1)} V^{(1)} = \rho^{(1)} \pi D^{(1)^3} \big/ 6 \\ E &= E_S{}^{(1)} + E_{KE}{}^{(1)} = \sigma^{(1)} A^{(1)} + \rho^{(1)} V^{(1)} \left(u^{(1)^2} + v^{(1)^2} + w^{(1)^2} \right) \big/ 2 \\ &= \sigma^{(1)} \pi D^{(1)^2} + \rho^{(1)} \pi D^{(1)^3} \left(u^{(1)^2} + v^{(1)^2} + w^{(1)^2} \right) \big/ 12 \end{aligned} \qquad (1)$$

In Eq. (1), E_S and E_{KE} denote the surface and kinetic energy of the droplet, respectively, where σ is the surface tension and D is the droplet diameter. The superscript (..) notation is to indicate properties of the droplet at a particular state (..) and is used throughout the paper. At impact state (2), the droplet is assumed to be roughly pancake in shape having

a maximum diameter equal to $D_{\max}$. At this state, the kinetic energy of the droplet is negligible and resuls in only a surface energy contribution to the total energy of the droplet [17],

$$E_S^{(2)} = \sigma\pi D_{\max}{}^2 \left(1-\cos\alpha\right)/4 \tag{2}$$

where α is the contact angle defined as the intersection of the tangent line at the liquid-vapor interface with the wall (see Figure 1). The diameter at state (2) may be determined through an energy balance by equating the pre-impact energy of the droplet at state (1) to the sum of the impact energy at state (2) and the lost work due to viscous dissipation.

$$E_S^{(1)} + E_{KE}^{(1)} = E_S^{(2)} + W \tag{3}$$

In Eq. (3), W is the work lost due to viscous dissipation as the droplet undergoes deformation from states (1) to (2) and may be approximated using the relation [7]:

$$W \cong \rho\pi\left|U\right|^2 D^3 \beta_{\max}{}^2 \Big/ \left(3\sqrt{\mathrm{Re}}\right) \tag{4}$$

where β_{MAX} is defined as the ratio of the maximum droplet diameter at impact to its original size at state (1), *i.e.*, $\beta_{MAX} = D_{MAX}/D$, and $\mathrm{Re}\,(=\rho D\left|U\right|/\mu)$ is the droplet Reynolds number. Substituting this expression for work along with the surface and kinetic energy definitions of Eqs. (1) and (2) into Eq. (3) allows for the following analytical result for β_{MAX} [7].

$$\beta_{MAX} = \sqrt{\left[12+We\right]\Big/\left[3\left(1-\cos\alpha\right)+4\left(We/\sqrt{\mathrm{Re}}\right)\right]} \tag{5}$$

Once β_{MAX} is determined, then the energy at state (2) is known and will be used for determining the energy at state (3). At state (3), one of three events is assumed to occur involving either droplet sticking, rebounding, or shattering. Droplet shattering is assumed if the Weber number, $We\,(=\rho D\left|U\right|^2/\sigma)$, exceeds a critical Weber number, We_C, expressed in terms of the Ohnesorge number, Oh $(=\sqrt{We}/\mathrm{Re}\,)$[2]:

$$We_C = 7.9x10^{10} Oh^{2.8} \tag{6}$$

If $We < 2^{1/3} We_C$, then the droplet is allowed to either rebound or stick to the surface. Recent experimental studies of molten metal droplets [14] suggest that, if the surface energy at state (2) is greater than the energy dissipated during impact, the droplet will rebound, otherwise the droplet will stick. This simple criterion for droplet rebound is employed by assuming that if $E_S^{(2)} < W$ then the droplet sticks to the surface and the parcel is removed from the calculation (*i.e.*, no dripping effects are taken into account). If $E_S^{(2)} > W$ then the droplet is assumed to rebound and the velocity components of the droplet are adjusted to satisfy the known kinetic energy at state (3''). As an example, normalized $E_S^{(2)}$ and W of a 1 mm HFE-7100 ($C_4F_9OCH_3$) are given in Fig. 2 as a function of impact velocity using Eqs. (2) and (4), and the thermophysical properties of HFE-7100 summarized in Table 1.

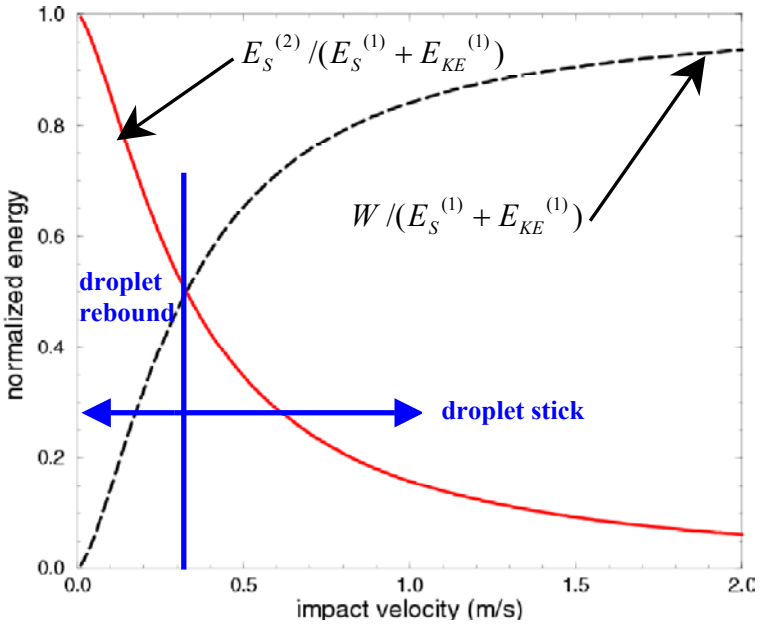

Figure 2: Normalized surface tension energy at state 2 and energy dissipated verses impact velocity for a 1 mm diameter HFE-7100 droplet.

In Figure 2, the surface energy and work are normalized by the total energy of the droplet at state (1). The droplet rebound occurs at low impact velocities (*i.e.*, less than 0.3 m/s) when the surface tension energy of the droplet at state (2) exceeds the amount of work required to deform the droplet. It is assumed that the difference in these quantities defines the kinetic energy of the droplet at state (3'').

$$E_{KE}^{(3'')} = E_S^{(2)} - W \tag{7}$$

Ideally, momentum conservation considerations of the droplet at impact would provide guidance for how the kinetic energy at state (3'') is distributed among the velocity components. Rather than pursue this approach, as a first step, a decrement factor, f, is introduced which reduces the velocity components at state (1) to match the kinetic energy state of the droplet at state (3'') using the following relations.

$$\begin{aligned} f^2 &= MIN(E_{KE}^{(3'')}/E_{KE}^{(1)},1) \\ u_{\parallel}^{(3'')} &= -f\,u_{\parallel}^{(1)} \\ u_{\perp 1}^{(3'')} &= f\,u_{\perp 1}^{(1)} \\ u_{\perp 2}^{(3'')} &= f\,u_{\perp 2}^{(1)} \end{aligned} \tag{8}$$

In Eq. (8) f is defined as the square root of the ratio of droplet kinetic energies at states (3'') and (1). This factor is multiplied by the velocity components of the droplet decomposed into a coordinate system aligned with the surface of impact, $(\hat{e}_{\parallel},\hat{e}_{\perp 1},\hat{e}_{\perp 2})$, as shown in Figure 3. The velocities, $u_{\parallel}$, $u_{\perp 1}$ and $u_{\perp 2}$ are the components of the droplet velocity in this new coordinate system decomposed into components parallel to the surface area vector and perpendicular to it, respectively.

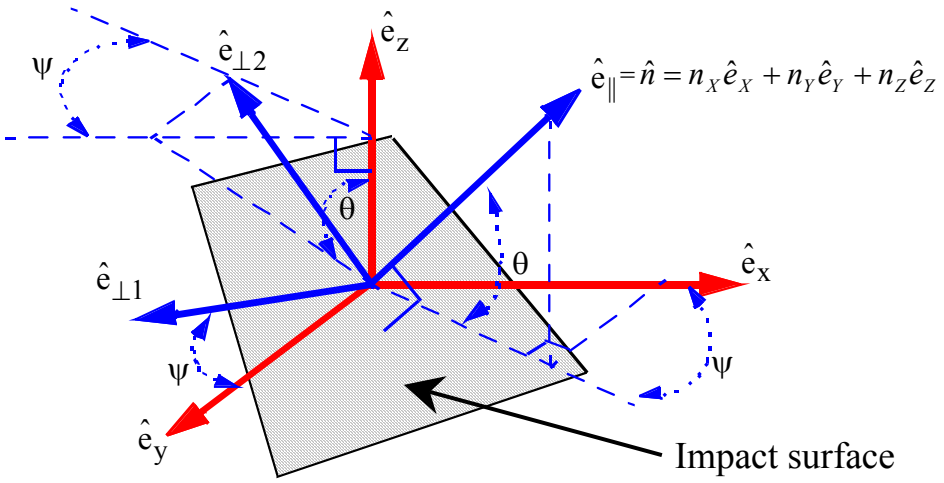

Figure 3: Relationship between impact surface and Cartesian coordinate systems.

The rebound boundary condition of Eq. (8) is implemented by first transforming the Cartesian velocities components of the droplet velocity at state (1) to the $(\hat{e}_{\parallel}, \hat{e}_{\perp 1}, \hat{e}_{\perp 2})$ coordinate system using the following transformation matrix:

$$\begin{Bmatrix} u_{\parallel}^{(1)} \\ u_{\perp 1}^{(1)} \\ u_{\perp 2}^{(1)} \end{Bmatrix} = \underline{\underline{T}} \begin{Bmatrix} u^{(1)} \\ v^{(1)} \\ w^{(1)} \end{Bmatrix} = \begin{bmatrix} \cos\theta\cos\psi & \cos\theta\sin\psi & \sin\theta \\ -\sin\psi & \cos\psi & 0 \\ -\sin\theta\cos\psi & -\sin\theta\sin\psi & \cos\theta \end{bmatrix} \begin{Bmatrix} u^{(1)} \\ v^{(1)} \\ w^{(1)} \end{Bmatrix} \tag{9}$$

where the direction angles θ and ψ are defined as:

$$\begin{aligned} \sin\theta &= \hat{e}_{\parallel} \bullet \hat{e}_Z \\ \cos\theta\sin\psi &= \hat{e}_{\parallel} \bullet \hat{e}_Y \\ \cos\theta\cos\psi &= \hat{e}_{\parallel} \bullet \hat{e}_Z \end{aligned} \quad . \tag{10}$$

Once the velocities at state (3'') are known from Eq. (8), then the velocities from the $(\hat{e}_{\parallel}, \hat{e}_{\perp 1}, \hat{e}_{\perp 2})$ coordinate system are transformed back to the Cartesian velocities using the following inverse transformation.

$$\begin{Bmatrix} u^{(3'')} \\ v^{(3'')} \\ w^{(3'')} \end{Bmatrix} = \underline{\underline{T}}^{-1} \begin{Bmatrix} u_{\parallel}^{(3'')} \\ u_{\perp 1}^{(3'')} \\ u_{\perp 2}^{(3'')} \end{Bmatrix} = \begin{bmatrix} \cos\theta\cos\psi & -\sin\psi & -\sin\theta\cos\psi \\ \cos\theta\sin\psi & \cos\psi & -\sin\theta\sin\psi \\ \sin\theta & 0 & \cos\theta \end{bmatrix} \begin{Bmatrix} u_{\parallel}^{(3'')} \\ u_{\perp 1}^{(3'')} \\ u_{\perp 2}^{(3'')} \end{Bmatrix} \tag{11}$$

Using Eqs. (8) through (11) allows for the determination of the velocities at state (3'') that is consistent with the known kinetic energy at that state. This procedure, however, is not unique and other approaches could be pursued. In practice, the details of how exactly the kinetic energy is distributed among the velocity components may not be important, since the inertia associated with the kinetic energy at state (3'') is much smaller than local drag forces. Future efforts will focus on better understanding the limitations of the decrement factor method for droplet rebound.

At still higher velocities, droplet shattering can occur. Two conditions need to be satisfied for droplet shattering. The first is the droplet Weber number at state (1) is larger than the critical Weber number. The second is at least two droplets must be formed at breakup. The combination of these two conditions leads to the following droplet breakup condition:

$$We \geq 2^{1/3} We_C \tag{12}$$

where We_C is the critical Weber number given in Eq. (6). If this condition is satisfied, then the size of the satellite droplets are assumed to be uniform in size and given as:

$$D^{(3''')} = MAX(\sigma^{(1)} We_C \big/ \rho^{(1)} |U^{(1)}|^2,\ D^{(1)^3} \pi\sigma \big/ E_S{}^{(1)}) \quad . \tag{13}$$

The first term in the MAX operator in Eq. (13) is the size of the droplet that would result if the Weber number was equal to the critical Weber number given the surface tension, density and velocity of the droplet at state (1). This estimate has been shown to be successful for predicting the size of satellite droplets from aerodynamic drag and is adopted here for estimates of the satellite droplet size at state (3''') [18]. In reality, a range of satellite droplet sizes is observed after a droplet shattering event, often exhibiting a lognormal distribution [19] which has been predicted with limited success using entropy principles [20,21]. These approaches are outside the scope of the current study. The second term in the MAX operator in Eq. (13) serves to impose a minimum droplet size for the satellite droplets. This limit is based on the fact that the sum of the surface energies from the satellite droplets at state (3''') has to be less than the surface energy of the parent droplet at state (2), *i.e.*, $N\sigma\pi D^{(3''')^2} < E_S{}^{(2)}$, where N is the total number of satellite droplets that is determined based on conservation of mass, $N^{(3''')} = (D^{(1)} \big/ D^{(3''')})^3$. The difference between $E_S{}^{(2)}$ and $N\sigma\pi D^{(3''')^2}$, divided by N, represents the kinetic energy imparted to each of the satellite droplets,

$$E_{KE}{}^{(3''')} = \left[E_S{}^{(2)} - N\sigma\pi D^{(3''')^2} \right] / N \quad . \tag{14}$$

The velocities resulting from droplet shattering are assumed to be equal in magnitude and determined from the kinetic energy at state (3''') using the following expressions:

$$\begin{aligned} u_{\parallel}{}^{(3''')} &= \sqrt{2E_{KE}{}^{(3''')} / 3} \\ u_{\perp 1}{}^{(3''')} &= 2\cos(2\pi RN)\sqrt{E_{KE}{}^{(3''')} / 3} \\ u_{\perp 2}{}^{(3''')} &= 2\sin(2\pi RN)\sqrt{E_{KE}{}^{(3''')} / 3} \end{aligned} \tag{15}$$

where RN is a random number between the values of 0 and 1. A random number is generated for every satellite droplet to create an azimuthally random distribution of droplets perpendicular to the surface of impact. Once the velocities in the transformed coordinate system are determined using Eq. (15), then the Cartesian values are assigned to the satellite droplets using the coordinate transformation of Eq. (11). As an example, the impact of 1 mm HFE-7100 droplets are considered in Figure 4. The size and number of the satellite droplets are given as a function of impact velocity. At low velocities, below 14 m/s, $We < 2^{1/3} We_C$ and no shattering is observed. At velocities greater than 14

m/s, the growth of satellite droplets quickly accelerates until an impact velocity of 65 m/s. Further increase in impact velocity beyond 65 m/s results in a more modest increase in satellite droplets as a minimum droplet size restriction is imposed from surface energy considerations (*i.e.*, the second term in the MAX operator of Eq. (13)).

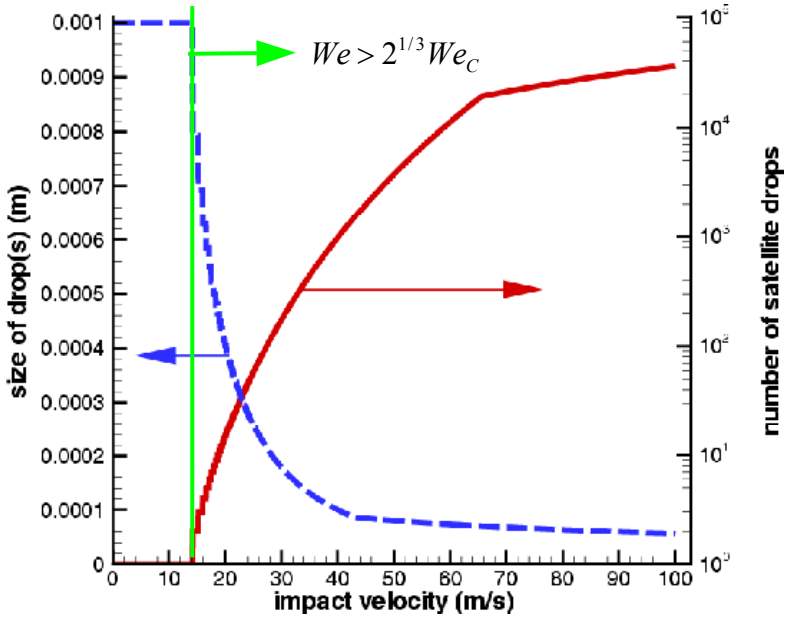

Figure 4: Size and number of satellite droplets as a function of impact velocity for 1 mm diameter HFE-7100 droplets.

RESULTS AND DISCUSSSION

The droplet impact model is implemented in the Sandia's fire physics code, VULCAN, as part of the Lagrangian dilute spray submodel. Further details of VULCAN and the spray model may be found in Ref. [22]. The objective of this work is to expand on the work of Ref. [23] to study the dispersion of HFE-7100 droplets around a cylinder in a homogeneous turbulent environment. The problem consists of grid-generated turbulent flow over a 32 mm diameter circular cylinder. Further details of the experimental arrangement and flow conditions may be found in Ref. [23]. The 3D CFD grid consists of a 26 x 51 x 80 grid for a total of 106,080 cells on a 0.772 m x 0.572 m x 0.914 m domain, as shown in Figure 5. A two-dimensional slice of the mesh in Figure 5 (b) shows local grid refinement in regions near the cylinder to better resolve the shear layers. The initial conditions of the calculation are chosen to best match the experiment by setting the inlet mean streamwise velocity, turbulence kinetic energy and its dissipation to values of 4.5 m/s, 0.304 m^2/s^2 and 0.0212 m^2/s^3, respectively. Figure 6 shows predictions of streamwise (a) mean and (b) RMS velocity for the case considered. Quantitative comparisons with experimental data in Ref. [23] showed that the numerical results over-predict the maximum streamwise mean velocity by 20 % and under-predict the RMS by 15 %.

In this study, 1 mm HFE-7100 ($C_4F_9OCH_3$) droplets are injected along the centerline of the domain and allowed to impact the cylinder. The thermophysical parameters of HFE-7100 needed for input to the spray model are available from the manufacturer, and summarized in Table 1. Three cases are considered that correspond to droplet injection velocities of 0.66, 2.1 and 21 m/s, respectively. These three velocities are chosen to result in droplet bouncing, sticking and shattering, respectively. Figures 7 through 9 show instantaneous snapshots of particle position and streamwise particle and gas-phase velocity for each case. For the first case, the velocity for most of the droplets just before impact is under 0.3 m/s, resulting in droplets bouncing off of the lower surface of the cylinder (see Fig. 2 for impact regime) and falling back to the inlet injection plane. In addition, some of the particles are entrained in the high-speed region near the cylinder surface and accelerated to velocities as high as 1 m/s. For the second case, the injection velocity is increased to 2.1 m/s resulting in an impact velocity of 1.85 m/s and droplet adhesion to the cylinder (see Fig. 2 for impact regime). For computational efficiency, particles that stick to the surface of the cylinder are presently removed from the calculation resulting in the array of droplets, as shown in Fig. 8. The injection velocity of the droplets is further increased to 21 m/s in the last case and results in droplet shattering. As indicated from Fig. 4, approximately 10 satellite droplets are generated for every parent droplet at this velocity. In this case, the diameter of satellite droplets is approximately 1/3 that of the parent droplets and they are readily entrained by the co-flowing air, as shown in Fig. 9.

CONCLUSIONS AND FUTURE WORK

In this study, a phenomenological particle impact model is formulated and implemented in the VULCAN fire physics code. The model is based on conservation of mass and energy principles along with breakup correlations for individual droplets. Three cases are run using 1 mm HFE-7100 droplets to explore the use of the model spanning impact regimes ranging from droplet bouncing to sticking to shattering. Future efforts using this model will compare code predictions to measurements of droplet size and velocity for spray impact on circular cylinders and other representative clutter objects using water and HFE-7100 agents.

ACKNOWLEDGEMENTS

This research is in part supported by the Department of Defense's Next Generation Fire Suppression Technology Program, funded by the DoD Strategic Environmental Research and Development Program. The authors would like to thank Dr. Dave Keyser acting on behalf of Naval Air Systems Command for coordinating this activity.

Table 1: Thermodynamic Parameters of HFE-7100 ($C_4F_9OCH_3$).

Property	*Value*
Molecular Weight	250 g/mol
Boiling Temperature	334 K
Critical Temperature	468.3 K
Heat of Vaporization @ B.P.	111.6 kJ/kg
Specific Heat @ room temperature	1183 J/kg
Density @ room temperature	1520 kg/m^3
Molecular viscosity	0.00061 kg/m-s
Surface Tension	0.0136 N/m

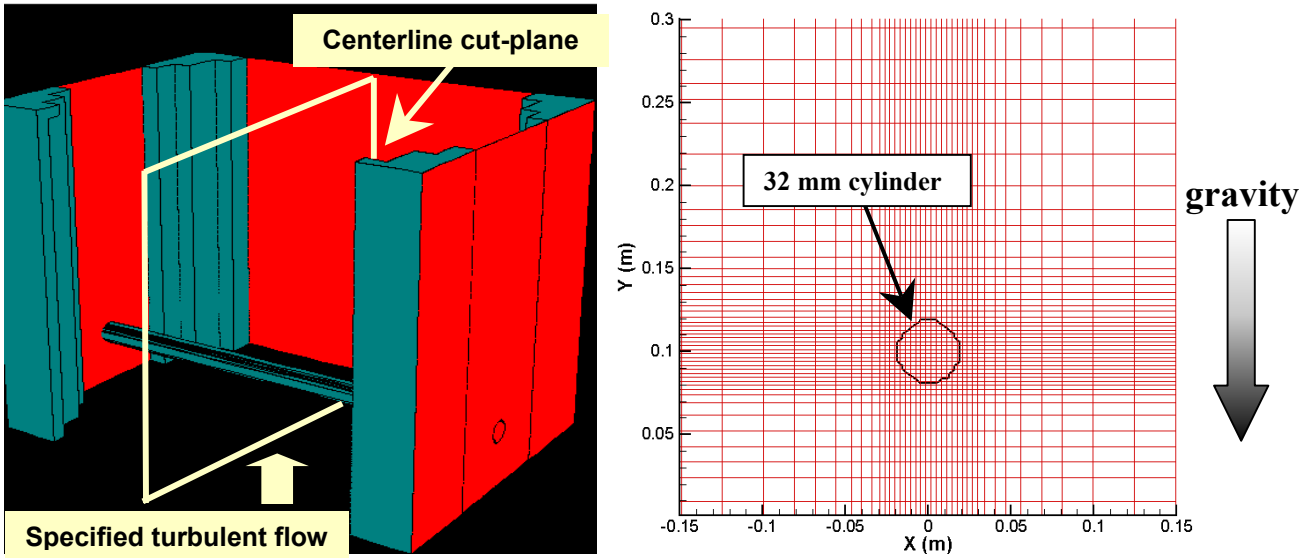

(a) (b)

Figure 5: Computational domain showing (a) outline of boundaries and cylinder and (b) the centerline grid.

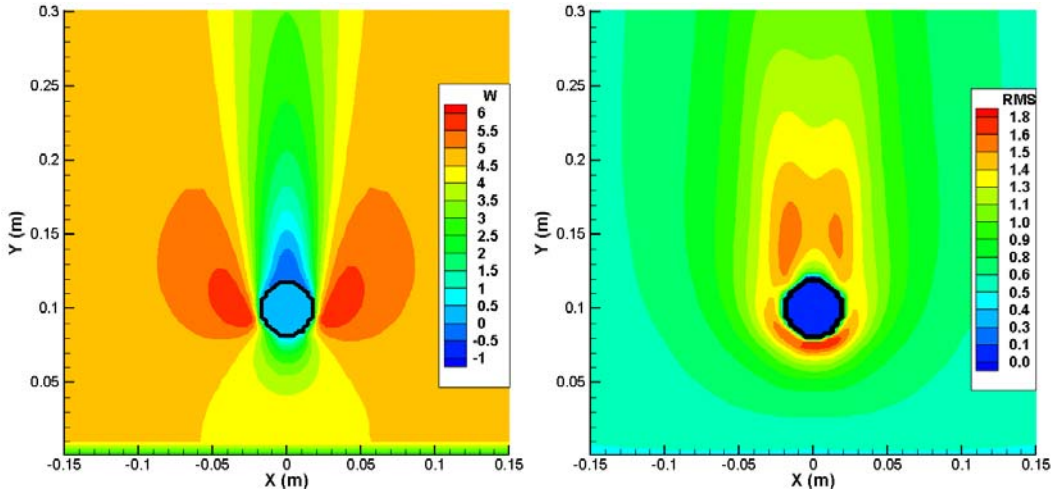

(a) (b)

Figure 6: Contour plots of streamwise (a) mean and (b) RMS velocity at centerline plane.

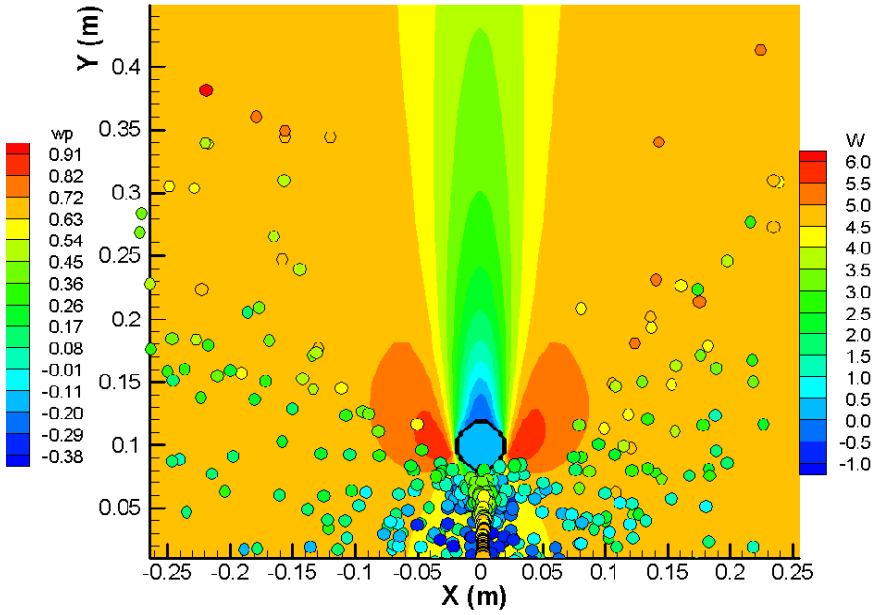

Figure 7: Instantaneous snapshot of 1 mm HFE-7100 droplets impacting circular cylinder at 0.66 m/s. W and wp are the mean and instantaneous streamwise velocities, respectively. Note, that the droplet sizes are exaggerated for clarity.

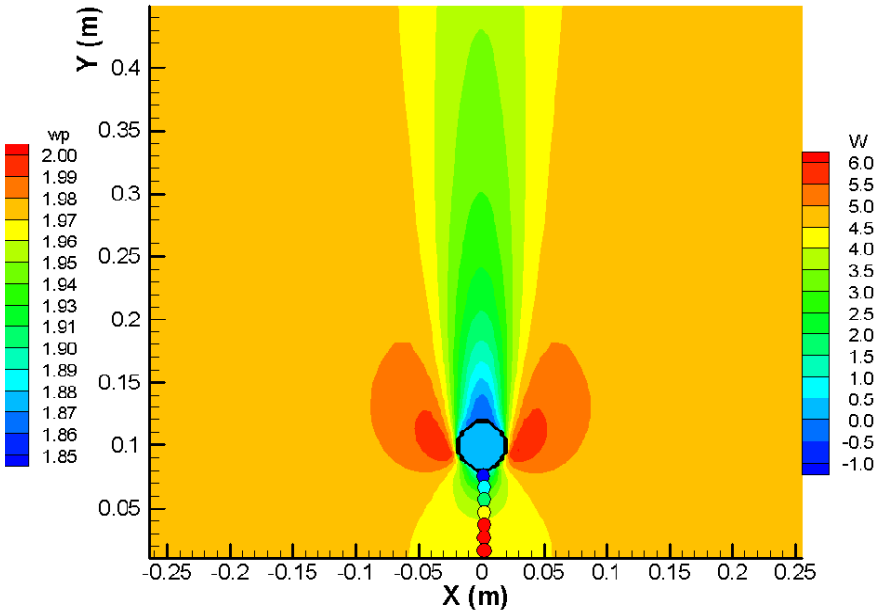

Figure 8: Instantaneous snaphot of 1 mm HFE-7100 droplets impacting circular cylinder at 2.1 m/s. W and wp are the mean and instantaneous streamwise velocities, respectively. Note, that the droplet sizes are exaggerated for clarity.

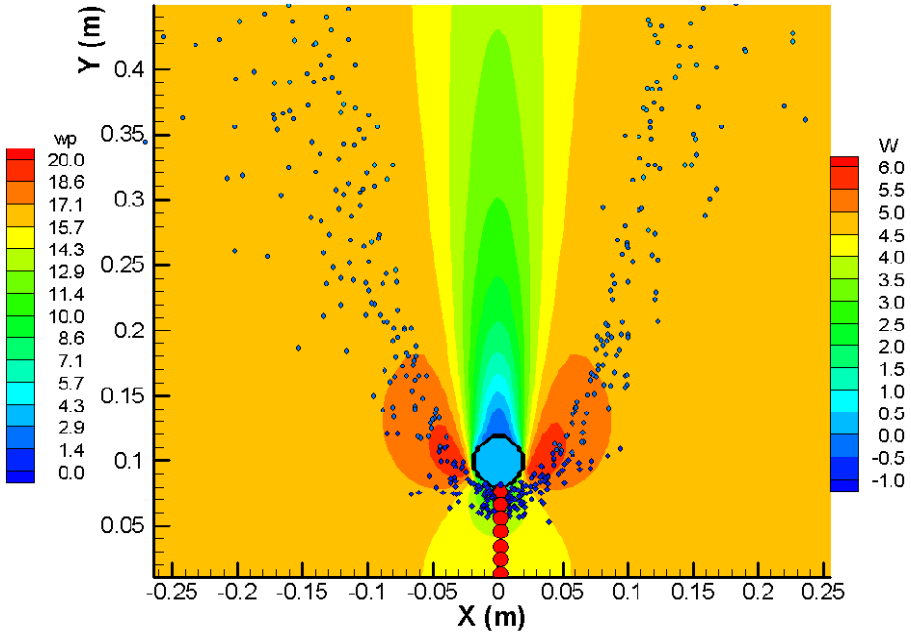

Figure 9: Instantaneous snapshot of 1 mm HFE-7100 droplets impacting circular cylinder at 21 m/s. W and wp are the mean and instantaneous streamwise velocities, respectively. Note, that the droplet sizes are exaggerated for clarity.

REFERENCES:

[1] Healy, W. M., Hartely, J.G. and Abdel-Khalik, S.I., "Comparison between theoretical models and experimental data for the spreading of liquid droplets impacting a solid surface," *Int. J. Heat Mass Transfer*, **39**, 3079-3082, 1996.

[2] Rein, M., "Phenomena of liquid drop impact on solid and liquid surfaces," *Fluid Dynamics Research*, **12**, 61-93, 1993.

[3] Foote, G.B., "The Water Drop Rebound Problem: Dynamics of Collision," *Journal of the Atomosphereic Sciences*, **32**, 1974.

[4] Tsurutani, K., Yao, M., Senda, J. and Fujimoto, H., "Numerical Analysis of the Deformation Process of a Droplet Impinging upon a Wall," *JSME Int. Journal*, **33**, 555-561, 1990.

[5] Fukai, J., Zhao, Z., Poulikakos, D., Megaridis, C.M. and Miyatake, O., "Modeling of the deformation of a liquid droplet impinging upon a flat surface," *Phys. Fluids*, **5**, 2588-2599, 1993.

[6] Fukai, J. Shiiba, Y., Yamamoto, T., Miyatake, O., Poulikakos, D., Megaridis, C.M. and Zho, Z., "Wetting effects on the spreading of a liquid droplet colliding with a flat surface: Experiment and modeling," *Phys. Fluids*, **7**, 236-247, 1995.
[7] Pasandideh-Fard, M., Qiao, Y.M., Chandra, S. and Mostaghimi, J., "Capillary effects during droplet impact on a solid surface," *Phys. Fluids*, **8**, 650-659, 1996.
[8] Bernardin, J.D., Stebbins, C.J. and Mudawar, I., "Effects of surface roughness on water droplet impact history and heat transfer regimes," *Int. J Heat and Mass Transfer*, **40**, 73-88, 1997.
[9] Hung, L.S. and Yao, S.C., "Experimental investigation of the impaction of water droplets on cylindrical objects," *Int. J. of Multiphase Flow*, **25**, 1545-1559, 1999.
[10] Bussmann, M., Mostaghimi, J. and Chandra, S., "On a three-dimensional volume tracking model of droplet impact," *Phys. Fluids*, **11**, 1406-1417, 1999.
[11] Chandra, S. and Avedisian, C.T., "On the collision of a droplet with a solid surface," *Proc. R. Soc. Lond. A*, **432**, 13-41, 1991
[12] Harvie, D.J.E. and Fletcher, D.F.,"A hydrodynamic and thermodynamic simulation of droplet impacts on hot surfaces, Part II: validation and application," *Int. J. of Heat and Mass Transfer*, **44**, 2643-2659, 2001.
[13] Pasanddideh-Fard, M., Bhola, R., Chandra, S. and Mostaghimi, J., "Deposition of tin droplets on a steel plate: simulations and experiments," *Int. J. of Heat and Mass Transfer*, **41**, 2929-2945, 1998.
[14] Aziz, S. D. and Chandra, S., "Impact, recoil and splashing of molten metal droplets," *Int. J. of Heat and Mass Transfer*, **43**, 2841-2857, 2000.
[15] Manzello, S. L. and Yang, J.C., "An experimental study of high weber number Impact of methoxynonaflourobutance C4F9OCH3 (HFE-7100) and n-heptane Droplets on a Heated Solid Surface," *Int. J. of Heat and Mass Trans*., accepted for publication, 2002.
[16] Manzello, S. L. and Yang, J.C., "On the collision dynamics of a Water Droplet containing an additive on a Heated Solid Surface," *Proc. Roy. Soc. London A.,* accepted for publication, 2002.
[17] Ford, R.E. and Furmidge, C.G.L., "Impact and spreading of spray drops on foliar surfaces," *Wetting*, *Soc. Chem. Industry Monograph*, 417-432, 1967.
[18] Pilch, M and Erdman, C. A., "Use of breakup time data and velocity history data to predict the maximum size of stable fragments for acceleration-induced breakup of a liquid drop," *Int. J. Multiphase Flow*, **13**, 741-757, 1987.
[19] Levin, Z. and Hobbs, P.V., "Splashing of water drops on solid and wetted surfaces: hydrodynamics and charge separation," *Phil. Trans. R. Soc. London A.,* **269**, 1971.
[20] Cohen, R. D., "Shattering of a liquid drop due to impact," *Proc. R. Soc. Lond.,* **435**, 483-503, 1991.
[21] Englman, R., "Fragments of matter from a maximum-entropy viewpoint," *J. Phys. Condens. Matter*, **3**, 1019-1053, 1991.
[22] DesJardin, P.E., Gritzo, L.A. and Tieszen, S. R., "Modeling the effect of water spray suppression on large-scale pool fires," *Proceedings of the Halon Options Technical Working Conference*, 262-273, 2000.
[23] Presser, C. and Widmann, J. F., DesJardin, P.E. and Gritzo, L.A., "Measurement and Numerical Prediction of Homogeneous Turbulent Flow over a Cylinder: A Baseline for Droplet-Laden Flow Studies," *AIAA paper*, AIAA 2002-0905, 2002.